

***Final Draft***

**of the original manuscript:**

Ebert, K.; Bengtson, G.; Just, R.; Oehring, M.; Fritsch, D.:

**Catalytically active poly(amideimide) nanofibre mats with high activity tested in the hydrogenation of methyl-cis-9-octadecenoate**

In: Applied Catalysis A (2008) Elsevier

DOI: 10.1016/j.apcata.2008.05.009

Catalytically active poly(amideimide) nanowebs with high activity tested in the hydrogenation of methyl-cis-9-octadecenoate

K. Ebert \*, G. Bengtson, R. Just, D. Fritsch

GKSS Research Centre Geesthacht GmbH, Institute of Polymer Research, Max-Planck-Str. 1, 21502 Geesthacht (Germany)

\* corresponding author ([katrin.ebert@gkss.de](mailto:katrin.ebert@gkss.de))

## Abstract

Nanofibres of poly(amideimide) (PAI) were prepared by electrospinning from solutions of 11 wt% PAI in dimethylformamide. Addition of small amounts of citric acid to the spinning solution improved the fibre size and fibre uniformity. Catalytical activation of the electrospun nanofibres was performed by applying an organic solution of palladium diacetate containing citric acid onto the fibres and subsequent thermally induced conversion to nanosized palladium clusters durably fixed on the fibres. These fibres were applied in the hydrogenation of methyl-cis-9-octadecenoate as a model reaction. The palladium-doped nanofibres showed a 2.5 times higher hydrogenation rate than a commercial palladium catalyst supported on alumina.

## 1. Introduction

Fibres with diameters in the submicron range offer a high surface-to-volume ratio and superior mechanical properties. This makes them interesting for several applications among them medical devices, releasing systems, tissue engineering, sensors, composites, textiles and catalysis.

A capable method for the preparation of nanofibres with diameters less than 100 nm is electrospinning either from polymer solutions or polymer melts [1-7]. In this process a polymer solution or polymer melt moves under the influence of a strong electric field between two electrodes. One of the electrodes often is a metallic capillary nozzle while opposite to it a grounded collecting electrode is situated. As the polymer solution or polymer melt leaves the nozzle a hemispherical droplet is formed. A conical shape of this droplet, the Taylor cone [8,9], is formed as the applied electric field is strong enough to overcome the surface tension of the polymer solution. If the molecular weight and the concentration of the polymer are sufficiently high entanglement of the polymer chains occurs and a fibre is formed [10,11,12]. The dimensions and morphologies of electrospun polymeric nanofibres can be influenced by a number of parameters such as strength of the electric field, spinning distance, nozzle diameter, polymer concentration, surface tension, conductivity and solvent [13-18].

In catalysis nanofibres may serve as supports for immobilised catalysts. High catalytic surface areas per volume units are possible by the nano size of the fibres. Even non-porous fibres may provide suitable catalyst surface areas to compete with traditionally supported, porous catalysts.

So far only a few paper dealing with that subject have been published. Demir et al. [19] studied the catalytic activity of palladium (Pd) nanoparticles on electrospun fibres of acrylonitrile and acrylic acid copolymers. For the hydrogenation of dehydrolinalool they found a 4.5 times higher catalytic activity for the nanofibrous system compared to a conventional Pd/Al<sub>2</sub>O<sub>3</sub> catalyst. Graeser et al [20]. developed catalytically active core-shell fibres. The core fibres containing noble metal salts were prepared by electrospinning while the shell of poly-p-xylylene (PPX) was deposited from the vapour phase. Reduction of metal salts was performed by thermal decomposition. For some fibres the core polymer was extracted leaving nanotubes with uniformly distributed metal nanoparticles at the inner tube walls. In model hydrogenation reactions it was shown that the configuration, i. e. core-shell fibres or nanotubes, had a significant influence on the reaction routes. Stasiak et al. [21] prepared core-shell nanofibres where the homogeneous catalyst scandium triflate was immobilised in the core. The results revealed that the leaching of catalyst in such systems is strongly influenced by the permeability of the shell material and the catalyst leaching diminishes the practicability in processes.

In our work we have focused on the immobilisation of Pd nanoparticles on electrospun nanofibres of poly(amideimide) (PAI), a polymer of high temperature stability (T<sub>g</sub>~280°C [22]). The PAI nanofibres were collected during spinning to mats and were further catalytically activated by a patented thermal treatment to yield perfectly fixed nano-sized catalyst on the surface of the nanofibres. The catalytical activity of these nanofibrous mats was tested in the hydrogenation of methyl-cis-9-octadecenoate (methyl oleate), a model compound for edible oil hydrogenation.

Previously, this reaction was studied with catalytically active membranes, where the Pd nanoparticles were immobilised in the pores of the membranes. One of the crucial aspects in the work was the development of high flux membranes to allow processing of rather high viscous liquids. An alternative to porous membranes could be nanofibrous mats with very low resistance to flow which is especially of great benefit if high viscous fluids have to be processed. Additionally, the high surface area of the nanofibres should enable a supported catalyst system with high catalytic activity.

## Experimental

*Materials.* Polyamideimide (Torlon HV from Solvay Advanced Polymers) was used as the fibre forming polymer. It was dissolved in DMF (Merck). Citric acid (Aldrich) and palladium diacetate ( $\text{PdAc}_2$ ) from Chempur were used as additives in the spinning solution.  $\text{PdAc}_2$  and Pd/alumina (5 % Pd, Merck) were stored under dry conditions. Methyl oleate (technical grade 65 % containing 4 % trans-isomer, 2 % saturated fatty ester, 10 % linolate, 19 % fatty esters of C12 to C16, Merck) was stored in the freezer and warmed up in small portions before use. All chemicals were used without further purification.

*Preparation of polymer solution.* PAI solutions were prepared by dissolving the proper amount of polymer in DMF. After receiving a homogeneous solution citric acid was added and the solution was stirred until the salt was dissolved. The solutions were filtered through a 32  $\mu\text{m}$  metal filter to remove possible agglomerates and undissolved species.

*Electrospinning* was performed with a set-up designed and constructed at GKSS. The polymer solution was fed through a steel needle with an inner diameter of 0.6 mm, which acted as the high potential electrode. The mass electrode consisting of steel was placed above the counter electrode realising bottom-to-top-electrospinning. The solution flow was adjusted to 30 ml/h with an infusion pump (Medipan Typ 610 BS, Poland). The experiments were performed at 27 kV or 26 kV and at a spinning distance of 30 cm or 25 cm. The electrospun fibres were collected on aluminium foil for 15 minutes.

*Characterisation of nanofibres:* Characterisation of the neat electrospun fibres was performed with a Leo 1550 VP Gemini<sup>®</sup> field emission scanning electron microscope from Zeiss Company at 3 kV. Samples were sputtered with a 2.5 nm thick layer of Au/Pd. Catalytically active nanofibres were carbon coated prior to analysis.

Field emission gun transmission electron microscopy analysis was performed with a Tecnai G<sup>2</sup> F20 from Fei Company operated at 200 kV. The nanofibres were transferred on a lacey carbon filmed grid and analysed without any treatment.

*Catalytic activation.* The activation solution was combined from 2 solutions. Solution 1 containing 0.1 g  $\text{PdAc}_2$  in 16 ml ethyl acetate (EtAc) and solution 2 composed of 0.8 g citric acid and 8 ml methanol (MeOH) (total: 0.5 %  $\text{PdAc}_2$  and 3.5 % citric acid in EtAc/MeOH 2:1). The nanofibre mats supported by non-woven were immersed in the clear orange activation solution for 1 minute, removed from the bath and allowed to dry in air for 1 hour. The nanofibre samples were wrapped for protection in additional technical non-woven, fixed in a metal frame and heated in air to 175 °C for 6 hours. The yellowish fibres turned into a light grey. For the analysis of the final Pd content the fibres were released from the non-woven by aid of MeOH and dried in vacuum at 50 °C. After weighing the fibres, 2 ml of aqua regia and a certain amount of  $\text{YCl}_3$  as internal standard were added and the flask was heated to 60 °C for 30

minutes. The yellow solution of dissolved Pd was separated from the fibres and the Pd-concentration was measured by Total Reflection X-ray Fluorescence (TXRF) [23]. *Test of catalytic activity (Methyl oleate test)*. A catalytically activated sample of 9.08 cm<sup>2</sup> non-woven supported activated nanofibres was fixed to a magnetic stirring bar with a small amount of glue. The stirring rate was limited by the set-up to 200 to 300 rpm. The thus fixed fibres were stirred in 30 ml n-decane at 100 °C and the solvent was bubbled with hydrogen for 1 - 2 hours to activate the Pd-catalyst. After addition of 1 g (2.2 mmol) methyl oleate to the solvent under constant feed of H<sub>2</sub> the hydrogenation started immediately. Samples of 0.5 ml were drawn regularly over a period of 3 hours, diluted with n-hexane (1:10) and analysed by gas chromatography (GC HP5890 II with FID and auto sampler, 100 m Supelco SP 2560 capillary column, carrier gas: Helium). The reaction was followed by taking 10 samples of 0.5 ml over a period of 3 hours. The supported Pd/Al<sub>2</sub>O<sub>3</sub> catalyst was suspended in n-decane and treated identically.

## Results and discussion

### Results of electrospinning

Electrospinning with solutions containing 9, 10 and 11 weight% (wt%) PAI revealed decreasing number of beads and increase in fibre uniformity with increasing polymer concentration (Figure 1). Nanofibrous mats obtained from the 9 wt% solution show a relatively high number of beads and randomly distributed thicker and thinner fibres (Table 1). Electrospinning of the 10 wt% PAI solutions resulted in fibres with only a few beads and relatively uniform diameters. With the 11 wt% spinning solutions fibres with rather uniform diameters were obtained. No beads could be observed.

The addition of citric acid to the spinning solution further improved the appearance of the nanofibres (Figure 2). Small amounts of the acid, i.e. 0.5 wt%, resulted in fibres with the lowest difference between minimum and maximum diameter (Table 1). With 1.5 and 2.5 wt% citric acid the appearance of thin fibres below 100 nm could be observed. Electrospinning with higher concentrations of citric acid, i.e. 4.3 wt% and 5.2 wt% citric acid in the polymer solution resulted in fibres with rough surfaces. The difference in minimum and maximum fibre diameter increased significantly. No fibres with diameters below 100 nm could be observed. These results may be conceived by a rise in solution viscosity and conductivity with increasing the concentration of citric acid in the spinning solution (Figure 3). Higher solution viscosities usually result in thicker and often less uniform fibres [13,15,24].

The rough surfaces of PAI fibres at higher citric acid concentrations can be attributed to the relatively high conductivity as it was already described by several authors [13].

### Catalytic activation of the nanofibrous mats

A high dispersion together with a perfect fixation is required for an efficient and durable heterogeneous catalyst. In former works it was shown that the dispersion and durability of noble metal catalysts directly on the surface of the inner pores of a porous, polymeric membrane can be improved by the addition of citric acid applying a thermal decomposition of the precursor salt directly on the polymer surface [25-27].

Dipping the electrospun nanosized fibre mats into an organic solution of PdAc<sub>2</sub> containing a high amount of citric acid, [28] subsequent drying in air and heat treatment at 175°C yielded a nanosized, durable Pd catalyst. This catalyst can be activated by H<sub>2</sub> at 1 bar and room temperature, only. The nanosize and the dispersion of the Pd on the outer surface of the nanofibres can be seen clearly either by SEM or TEM (Figures 4,5). In the SE mode the Pd-clusters are visible as small spots on the surface of the fibres. These spots are visible as bright dots of 5-12 nm size on back scattered electron (BSE) images. Because the fibres are thin enough they can be analyzed in addition directly by TEM. Here also smaller clusters are visualized. The sizes detected vary between about 2 and 10 nm with a maximum of distribution at around 3-5 nm. Some of the clusters are arranged alongside of channels one beside the next. This conformation may be the result of cavities on the surface of the fibres during the spinning process, causing a higher concentration of the activation solution, and, therefore, of clusters on this particular part of the surface

### Results of hydrogenation

The hydrogenation of methyl-cis-9-octadecenoate (methyl oleate) may proceed directly to the product methyl stearate or may be first rearranged to the trans-isomer methyl-trans-9-octadecenoate (methyl elaidate) and then react to the final product (see Scheme 1). In the Pd catalysed hydrogenation direct reaction of methyl oleate to methyl stearate is negligible and the hydrogenation proceeds via trans-rearrangement to the product [25].

Figure 6 displays a typical hydrogenation experiment applying nanofibre mats activated with Pd nanoclusters. With proceeding reaction a steady decrease of oleate and a steep increase of the intermediate elaidate is seen together with a slow, delayed onset of stearate increase. This supports the reaction route to proceed principally via the isomerisation route and not directly. After reaching a considerable concentration of elaidate (trans) a linear increase of product formation of stearate at a rate of 0.77 mmol/h mgPd is calculated.

For comparison a hydrogenation reaction was performed with a commercial Pd/Al<sub>2</sub>O<sub>3</sub> catalyst. As can be seen from Figure 7 the reaction proceeds similar, except the product stearate is formed without any delay indicating that probably also direct hydrogenation from oleate occurs. The hydrogenation rate of methyl stearate was determined as 0.3 mmol/h mgPd.

Comparison of the hydrogenation rates reveals that the reaction with the catalytically active nanofibres this is about 2.5 times faster than with the commercial Pd/Al<sub>2</sub>O<sub>3</sub> catalyst. The catalytic activity of the nanofibres probably could be even higher since the presently used experimental procedure may not assure a sufficient flow through the mats for optimal catalyst contact by only being stirred. An improved apparatus will be build to ensure optimal flow through conditions to exclude this possible drawback in further tests.

### Acknowledgement

Marion Aderhold and Clarissa Abetz are kindly acknowledged for the SEM and TEM analyses.

Dr. Simone Griesel is kindly acknowledged for the TXRF analyses.

## References

- [1] A. Formhals, US Patent 1,975,504 (1934).
- [2] Z.-M. Huang, Y.-Z. Zhang, M. Kotaki, S. Ramakrishna, *Composites Science and Technology*, 63 (2003) 2223-2253.
- [3] D. Li, Y. Xia, *Adv. Mater.* 16, (2004) 1151-1170.
- [4] S. Ramakrishna, K. Fujihara, W.E. Teo, T. Yong, Z.W. Ma, R. Ramaseshan, *Materials Today* 9(3) (2006) 40-50.
- [5] D.H. Reneker, A.L. Yarin, E. Zussman, H. Xu, *Advances in Applied Mechanics* 41 (2007) 43-195.
- [6] A. Greiner, J.H. Wendorff, *Angewandte Chemie-International Edition* 46(39) (2007) 5670-5703.
- [7] R. Dersch, M. Graeser, A. Greiner, J.H. Wendorff, *Australian Journal of Chemistry* 60(10) (2007), 719-728.
- [8] G. Taylor, *Proc. Roy. Soc. Lond. A* 280 (1964) 383-397.
- [9] G. Taylor, *Proc. Roy. Soc. Lond. A*. 313 (1969) 453-475.
- [10] A. Koski, K. Yim, S. Shivkumar, *Materials Lett.* 58 (2004) 493-497.
- [11] M.G. McKee, T. Park, S. Unal, I. Yilgor, T. E. Long, *Polymer* 46, (2005) 2011-2015.
- [12] Z. Jun, H.Q. Hou, J.H. Wendorff, A. Greiner, *E-Polymers Art. No.* 038 (2005).
- [13] J.M. Deitzel, J. Kleinmeyer, D. Harris, N. C. Beck Tan, *Polymer* 42 (2001) 261-272.
- [14] Z. Jun, H.Q. Hou, A. Schaper, J.H. Wendorff, A. Greiner, *E-Polymers Art. No.* 009 (2003).
- [15] H. Fong, I. Chun, D. H. Reneker, *Polymer* 40 (1999) 4585-4592.
- [16] R. Jaeger, M.M. Bergshoef, C. Martin i Baille, H. Schönherr, G.J. Vancso, *Macromol. Symp.*, 127 (1998), 141-150.
- [17] S. A. Theron, E. Zussman, A. L. Yarin, *Polymer* 45 (2004) 2017-2030.
- [18] C. L. Casper, J. S. Stephens, N. G. Tassi, D. B. Chase, J. F. Rabolt, *Macromolecules* 37(2) (2004) 573-578.

- [19] M. M. Demir, M. A. Gulgun, Y. Z. Menciloglu, B. Erman, S. S. Abramchuk, E. E. Makhaeva, A. R. Khokhlov, V. G. Matveeva, M. G. Sulman, *Macromolecules* 37 (2004) 1787-1792.
- [20] M. Graeser, E. Pippel, A. Greiner, J.H. Wendorff, *Macromolecules* 40 (2007) 6032-6039.
- [21] M. Stasiak, A. Studer, A. Greiner, J. H. Wendorff, *Chem. Eur. J.* 13 (2007) 6150-6156.
- [22] Y. Wang, S.H. Goh, T.-S. Chung *Polymer* 48 (2007) 2901-2909.
- [23] A. Prange, *Spectroc. Acta Pt. B-Atom Spectr.* 44 (1989) 437-452.
- [24] J. Doshi, D.H. Reneker *J. Electrostatics* 35(2-3) 1995 151-160.
- [25] D. Fritsch, G. Bengtson, *Catalysis Today* 118 (2006) 121-127.
- [26] G. Bengtson, D. Fritsch *Desalination* 200(1-3) (2006) 666-667.
- [27] D. Fritsch, G. Bengtson *Adv. Eng. Materials* 8(5) (2006) 386-389.
- [28] P. Papageorgiou, D.M. Price, A. Gavriilidis, A. Varma, *J. Catal.* 158 (1996) 439-451.

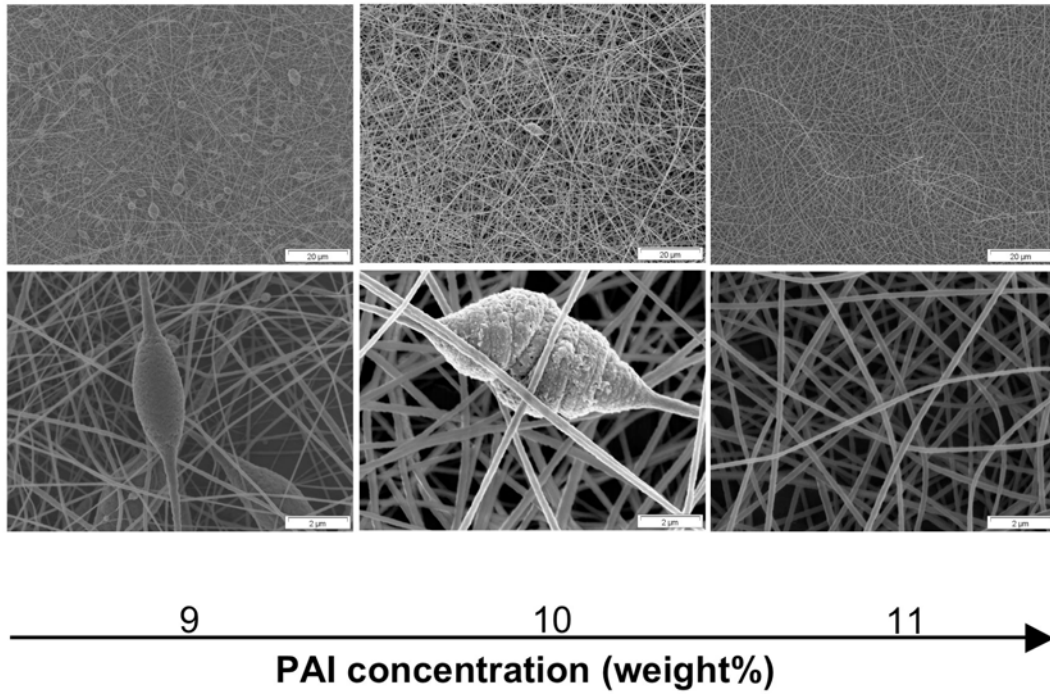


**Figure 1.** Influence of PAI concentration on morphology and dimensions of electrospun fibres.

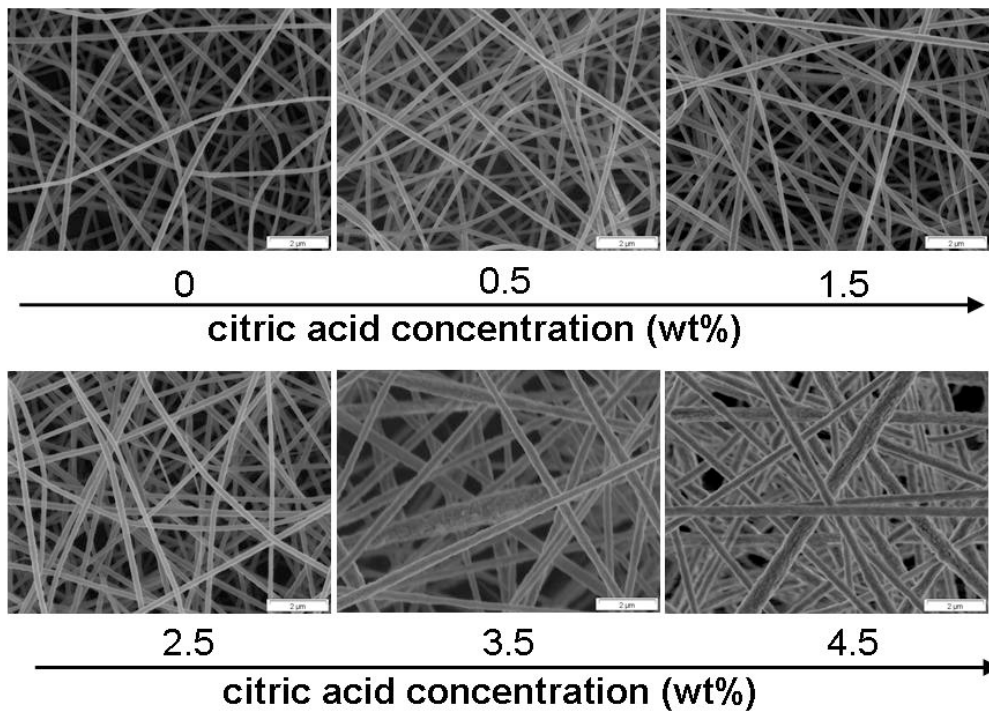


**Figure 2.** Influence of citric acid concentration on the morphology and dimensions of electrospun PAI fibres. (PAI concentration: 11 wt%)

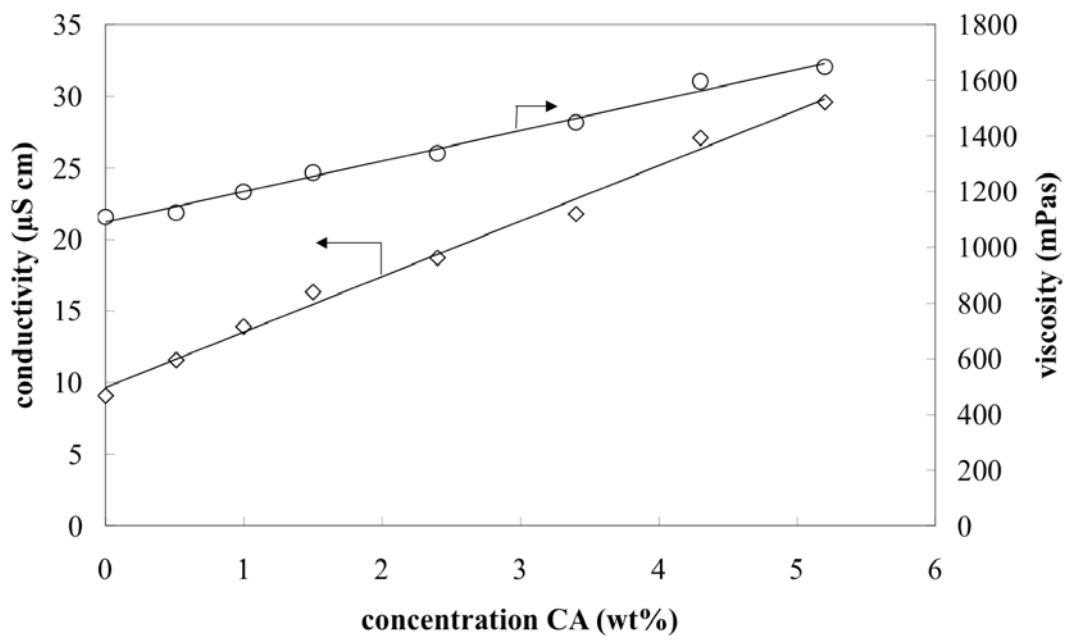


**Figure 3.** Viscosity and conductivity of PAI solution with increasing concentration of citric acid

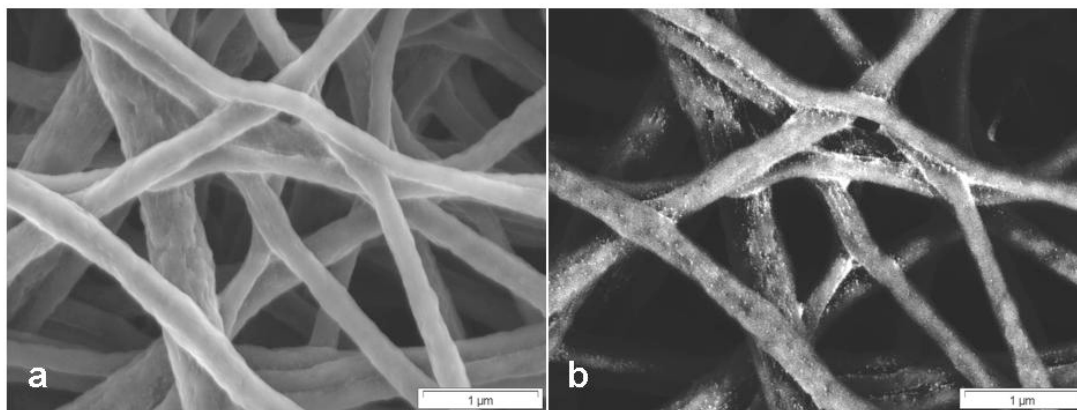


Figure 4 Scanning electron micrographs of Pd-doped PAI nanofibres: a) SE image b) BSE image

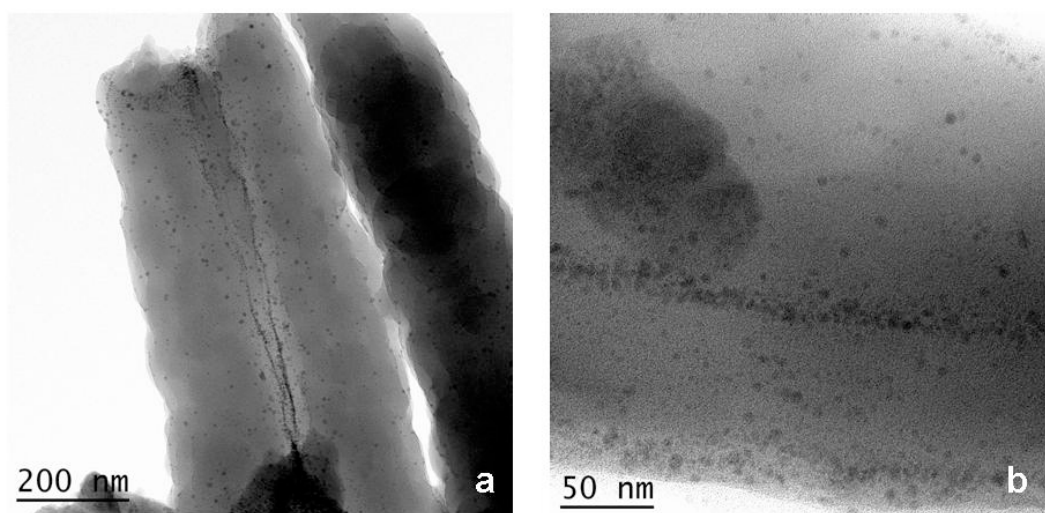
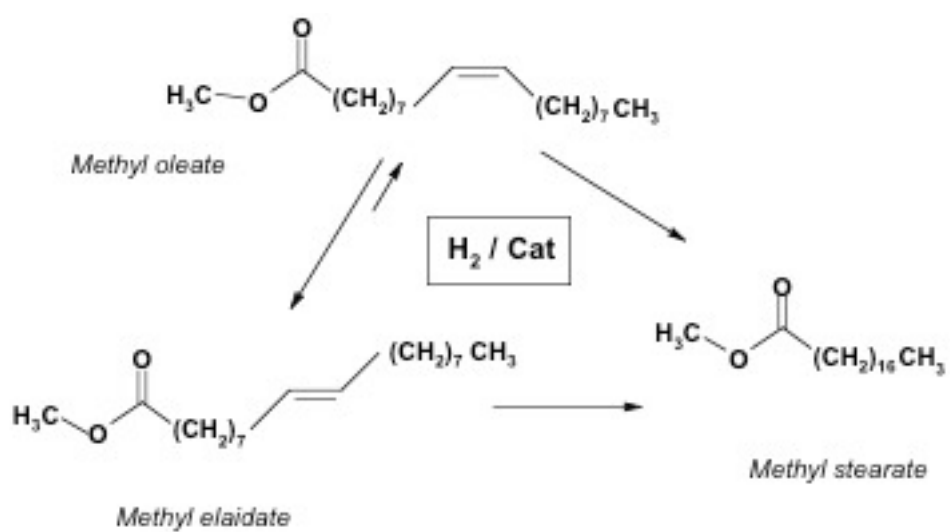
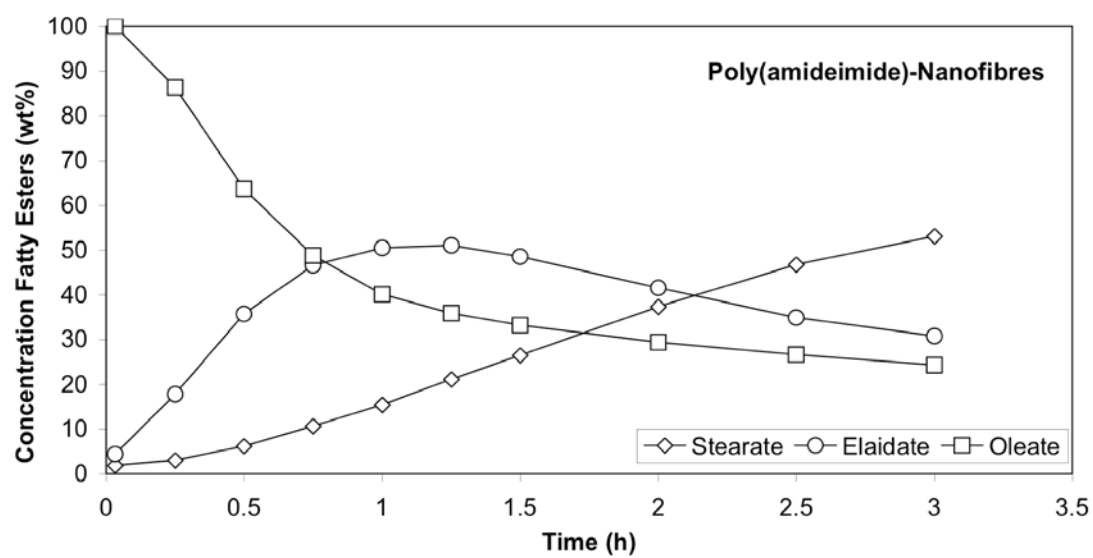


Figure 5 TEM micrographs of Pd-doped PAI nanofibres



**Scheme 1.** Reaction scheme of possible hydrogenation paths of methyl oleate



**Figure 6.** Hydrogenation of methyl oleate with PAI nanofibres doped with Pd nanoparticles.

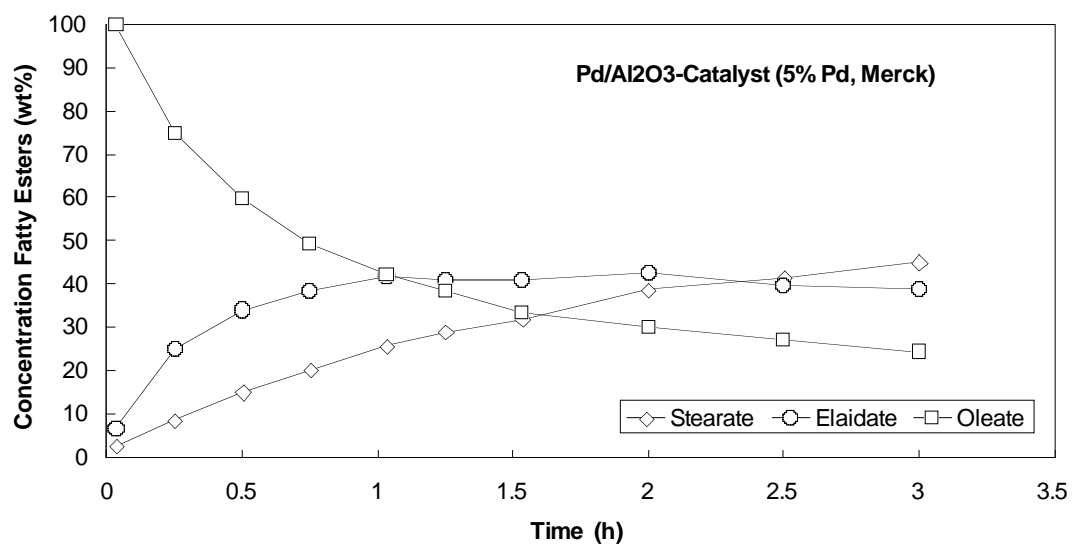


Figure 7. Hydrogenation of methyl oleate with a commercial supported Pd-catalyst.

## Tables

Table 1 Minimum and maximum diameters of electrospun fibres dependent on the concentration of citric acid

Concentration CA (wt%)	Minimum diameter (nm)	Maximum diameter (nm)	Difference of variation (nm)
0	167	325	158
0.5	117	246	129
1.5	58	283	225
2.5	78	268	190
3.5	215	950	735
4.5	284	791	507